International Journal of Nanoelectronics and Materials

In Press, Accepted Manuscript – Note to users

Electronic and Optical Properties of GaAs Armchair Nanoribbons: DFT Approach

Bramha P. Pandey[1,*]

[1]*Department of Electronics & Communication Engineering, MMMUT, Gorakhpur(U.P)-273010.*

[*]*Corresponding author: E-mail: pandey.bramha@gmail.com*

The electronic and optical properties of N atom width (N: 4, 8, 12, 16)armchair GaAs nanoribbons (NA GaAs NRs) have been studied with hydrogen(H)passivated nanoribbon using DFT approach. The H passivated edge of NA GaAs NRs with different width of nanoribbons provide great flexibility to modulate fundamental bandgap. All investigatedwidth of 4, 8, 12, and 16atom GaAs NRs are found to be semiconducting with direct bandgap having 3.071, 2.275, 2.155, and 2.02 eV respectivelyat k-point Z (0, 0, 0.5) which exhibit interesting width dependent (N: 4~12) behaviourof bandgap. The complex dielectric constant has been calculated with the use of Kubo-Greenwood formula from which refractive index(n(ω)) and absorption coefficient ($\alpha(\omega)$)have also been calculated for bulk as well asall width of GaAs armchair nanoribbons.The n_{zz} and α_{zz} components significantly play the major role to tune the refractive index and optical absorption coefficient of the GaAs nanoribbon.

KeywordsNanoribbon(NR), Armchair, DFT, MGGA, absorption coefficient, refractive index, bandgap

PACS Nos68.65.-k, 68.35.bg, 73.61.Ey, 74.25.Gz, 74.25.Jb, 81.07.Bc

1. Introduction

Two-dimensional (2D) materials such as graphene and others variant of graphene are playing a vital and exciting role in thefield of high-speednanodevices from last decade[1]–[3]. In particular, graphene has attracted great interest because of its unique properties such as pristine graphene exhibits metallic behavior with no band gap, whereas modified graphene can have afinitebandgap. As the band gap is critical to devices such as switching diode, light emitting diode,photodetector and solar cells. Different approaches have been adopted on graphene to modulate the bandgap, such as graphene nanoribbon synthesis[4], bilayer control [5], [6] and chemically modified graphene[7]–[9] However, most of these efforts have failed to achieve a significant variation in theband gap of graphene[10]. The 2D non-graphene materials, including layered, non-layered, and their heterostructures are presentlyappealingincreasingattention due to their favorable applications in electronics, optoelectronics and clean energy and nanodevices [11], [12]. 2D non-graphene materials are fabricated with same efficiency and performance as graphene and open a new dimension for research such as the monolayer transition metal disulfide (TMD), which are the likely and complement materials of the graphene[13]–[17].

Recently, wavy GaAs nanoribbons are fabricated onto a strained soft substrate to investigate the strain–photonic coupling effect[18], [19]. The electronic and transmission properties of low buckled GaAs nanoribbon have been investigated[20].In present work, we report the first-principles calculation of band gap modulation and optical properties such as refractive index and absorption coefficient in NA GaAs NRs by passivating the nanoribbon edges with hydrogen atomsusing density functional theory (DFT). To engineering, the band structure, and optical properties, boundary modification of the nanoribbons arenecessarily a promising and vital option. The most commonly used edge passivation is hydrogenation. The As edge of NA GaAs NRs is passivated with hydrogen atom, which leads to the bonding of As atoms at the edges different with other As atoms bonded with Ga. As consequences, the bond lengths of As-H at edges are shorter than that in middle of GaAs ribbons, and open the energy gaps of armchair NA GaAs NRs.The dangling bonds

at the armchair edges playa vitalrole in governing the electronic and optical properties. The rate oftheside of nanoribbon hydrogenation determined by temperature, pressure, and concentration of H_2 in the passivation process[21]. The most favourable condition (i.e., As edges are terminated with H) have been consider for the hydrogenation of the NA GaAs NRs. When nanoribbon is passivated with hydrogen atom, excess As which can be present either in elemental form or as an oxide As_2O_3 can be removed by the reaction mechanism[22]. The objective of this study is to design hydrogen(H) passivated armchair GaAs nanoribbons to analyse the electronic(bandgap and band structure), and optical (Refractive index, and Absorption coefficient) properties of armchair GaAs nanoribbons taking into the consideration of four different width (N: 4, 8, 12, and 16) of nanoribbons.

2. Computational Details

The armchair GaAs nanoribbon structures can view as tailoring a GaAs crystal in (100) Miller direction with padding of 10Åvacuum in x and y-direction while z is periodic and perpendicular to the armchair direction. Accordingly, the so-called armchair GaAs nanoribbon (NA GaAs NRs) can be identified by the number of layers of atoms across the ribbon width and are label as NA GaAs NRs. In this work, we focus on the armchair type and Fig. 1 shows the ball-and-stick model of NA GaAs NRs. We consider four different NA GaAs NRs with N = 4, 8, 12, and 16, which correspond to a width of 5.65 Å, 11.31 Å, 16.96 Å, and 22.61 Å, respectively. Upon structural relaxations, the lattice constants along the periodic direction are calculated to be 4.05 Å, 3.99 Å, 3.98 Å and 3.96 Å, respectively. The atomic structure of NA GaAs NRs is showing the low-buckled honeycomb lattice structure after the relaxation of the unit cell[23]. The relaxation calculations were carried out using first principles density functional theory (DFT) implemented in thequantum espresso source code[24]. The interaction between electrons and ions defined by Perdew-Burke-Ernzerhof (PBE) exchange-correlation functional [25] and theultrasoftpseudopotential (USPP) [26]. The kinetic energy cutoff and charge density cutoff for the plane wave basis set were chosen to be 50 Ry and 650 Ry respectively. The energy convergence criteria for electronic and ionic iterations were set to be 10^{-6} eV and 10^{-4} eV, respectively. The force convergence threshold was selected 10^{-3} eV/Å in ionic relaxation of the atoms for NA GaAs NRs. The reciprocal space was meshed at $1 \times 1 \times 16$ for the NA GaAs NRs using Monkhorst Pack meshes centered at Γ point[27]. A vacuum space of at least 10 Å was included in the unit cell to minimize the interaction between the system and itsperiodic replicas resulting from the periodic boundary condition. The electronic and optical properties of therelaxedstructure of NA GaAs NRs were calculated using meta GGA(MGGA) method implemented in thequantum-wise simulation tool[28]. MGGA functional combined with Tran and Blaha (TB09) method is a semi-empirical approach to accurately predict the electronic band structureand optical spectrum of the materials[29]. The calculation of electronic and optical properties requires a good description of virtual states far above the Fermi level. Therefore, we use the Hartwigsen, Goedecker, Hutter (HGH) pseudopotentials[30] with 4 Tier basis function for all atoms present in theunit cell. The K-points sampling and density mesh cutoff for basisfunctions were selected 1x1x64 Monkhorst Pack mesh grid and 100 Ha respectively. The 1x1x128 K-points mesh included in band structure and optical spectrum calculations.

3. Results and Discussion

3.1 Electronic properties calculation

All the calculations have performed after optimization of the unit cell of different width of NA GaAs NRs passivated with ahydrogen atom. The calculated bandgap of bulk zincblende GaAs was found 1.41 (1.42) eV using MGGA functional by setting the empirical parameter c=1.162. The value of theempirical parameter(c) calculated usingself-consistent DFT calculations employed in ATK-DFT code. A GaAs NRs confined in two dimensions and periodic in thez-direction. Therefore the unit cellbecomesanisotropicstructure. Due to change in structure from isotropic (bulk GaAs) to anisotropic(NA GaAs NRs), the valence band maximum and conduction band minimum k-point shifted to Z from Γ.It is interesting to note that atZ, there is valence band maximum and conduction

band minimum, term as direct bandgap shown in Fig. 2(a, b). The direct bandgap of all studied NA GaAs NRs are calculated and tabulatedin Table 1. There is plausible flexibility to tune the NA GaAs NRs bandgap by changing the width of the GaAs nanoribbons.

3.2 Optical properties calculation

The optical properties have beencalculated with the calculation susceptibility tensor, $\chi(\omega)$ by using the Kubo-Greenwood formula[31]. The relative dielectric constant,$\epsilon_r(\omega)$, polarizability, $p(\omega)$, and optical conductivity, $\sigma(\omega)$, are related to the susceptibility,$\chi(\omega)$ as
$\epsilon_r(\omega) = \big(1 + \chi(\omega)\big),\ p(\omega) = V\epsilon_0\chi(\omega),\quad and\ \sigma(\omega) = -i\omega\epsilon_0\chi(\omega)$, respectively[32].
The refractive index, n, is related to the complex dielectric constant through

$$n + ik = \sqrt{\epsilon_r}$$

where refractive index and extinction coefficients are n and k, respectively. The n and krepresentedin the form of real (ϵ_1) and imaginary (ϵ_2) components of the complex dielectric constant as

$$n(\omega) = \sqrt{\frac{\sqrt{\epsilon_1^2+\epsilon_2^2}+\epsilon_1}{2}} \text{and} \qquad k(\omega) = \sqrt{\frac{\sqrt{\epsilon_1^2+\epsilon_2^2}-\epsilon_1}{2}}$$

The optical absorption coefficient is representated in the form of the extinction coefficient (k) through

$$\alpha(\omega) = 2\left(\frac{\omega}{c}\right)k$$

where the speed of light, angular frequency, and extinction coefficient are c, ω, and k, respectively[33].
From the optimized structure of bulk zincblede GaAs, we calculated the refractive index, n(ω) and optical absorption coefficient, $\alpha(\omega)$ as function of incident photon wavelength(λ) shown in Figure 3. The calculated average values of refractive index, n(ω) over whole range of wavelength is ~3.1(experimental 3.2[34]) of bulk zincblende GaAs. There is noticeable results that n(ω) and $\alpha(\omega)$ are equal in all directions because of bulk GaAs is an isotropic and periodic crystal.The NR GaAs NRs were optimized and calculated the n(ω) and $\alpha(\omega)$ as function of incident photon λ shown in Figs. 4, 5, 6 and 7 respectively for all widths N: 4, 8, 12, and 16. For all widths of GaAs NRs, the average refractive index is~1.5. The n(ω) and $\alpha(\omega)$ are become anisotropic crystal due to confined in x and y-direction and periodic in thez-direction. We found different values of n(ω) in n_{xx}, n_{yy}, and n_{zz} direction for all four nanoribbon widths. Similarly, $\alpha(\omega)$ is the combination of all three different direction components such as $\alpha_{xx}, \alpha_{yy}\ and\ \alpha_{zz}$ for all four nanoribbon widths. It was also observed that as the nanoribbon width increases from 4 to 16, the z –direction components become more dominating compare to other two components of n(ω) and $\alpha(\omega)$. It is happening because of all NA GaAs NRs are periodic in z-direction and sufficient vacuum padded in x and y-direction so that periodic replicas of structurecannot interact to each other. The modulation of n(ω) and $\alpha(\omega)$ are possible by changing the width of NA GaAs NRs. The n_{zz} and α_{zz} components significantly play the major role to tune the refractive index and optical absorption coefficient of the GaAs nanoribbon.

4. Conclusion

In present work, hydrogen(H) passivated armchair GaAs nanoribbons have been designed and the electronic and optical properties of NA GaAs NRs have been calculated with the help of DFT theory. The modulation of the bandgap is possible by varying the width of the NA GaAs NRs as shown in Table 1. The optical properties have been calculatedusing Kubo-Greenwood formula from which refractive index and absorption coefficient have been calculated for bulk as well as all widths of GaAs armchair nanoribbon.The refractive index,n(ω) and optical absorption coefficient,$\alpha(\omega)$ of the GaAs nanoribbon can be significantly modulated by varying the widths of GaAs nanoribbons.

In Press, Accepted Manuscript – Note to users

The most governing component of the refractive index and optical absorption coefficient are n_{zz} and α_{zz}, respectively.

Acknowledgement
The author would like to thank IUAC, Delhi and C-DAC, Pune for providing the high performance computing facility available at IUAC and C-DAC center for this research article.

References

[1] Y. Zhu *et al.*, "Graphene and graphene oxide: Synthesis, properties, and applications," *Adv. Mater.*, vol. 22, no. 35, pp. 3906–3924, 2010.
[2] A. Splendiani *et al.*, "Emerging photoluminescence in monolayer MoS2," *Nano Lett.*, vol. 10, no. 4, pp. 1271–1275, 2010.
[3] F. Bonaccorso, Z. Sun, T. Hasan, and A. C. Ferrari, "Graphene Photonics and Optoelectronics," *Nat. Photonics*, vol. 4, no. 9, pp. 611–622, 2010.
[4] J. Cai *et al.*, "Atomically precise bottom-up fabrication of graphene nanoribbons," *Nature*, vol. 466, no. 7305, pp. 470–473, 2010.
[5] T. Ohta, "Controlling the Electronic Structure of Bilayer Graphene," *Science (80).*, vol. 313, no. 5789, pp. 951–954, 2006.
[6] J. B. Oostinga, H. B. Heersche, X. Liu, A. F. Morpurgo, and L. M. K. Vandersypen, "Gate-induced insulating state in bilayer graphene devices," *Nat. Mater.*, vol. 7, no. 2, pp. 151–157, 2008.
[7] X. Dong *et al.*, "Symmetry breaking of graphene monolayers by molecular decoration," *Phys. Rev. Lett.*, vol. 102, no. 13, 2009.
[8] K. Novoselov, V. Fal, and L. Colombo, "A roadmap for graphene," *Nature*, vol. 490, no. 7419, pp. 192–200, 2012.
[9] D. C. Elias *et al.*, "Control of graphene's properties by reversible hydrogenation: evidence for graphane," *Science (80-.).*, vol. 323, no. 5914, pp. 610–613, 2009.
[10] K. Kim, J.-Y. Choi, T. Kim, S.-H. Cho, and H.-J. Chung, "A role for graphene in silicon-based semiconductor devices.," *Nature*, vol. 479, no. 7373, pp. 338–44, 2011.
[11] F. Wang *et al.*, "Synthesis, properties and applications of 2D non-graphene materials," *Nanotechnology*, vol. 26, no. 29, p. 292001, 2015.
[12] B. Santhibhushan, M. Soni, and A. Srivastava, "Optical properties of boron-group (V) hexagonal nanowires: DFT investigation," *Pramana – J. Phys.*, vol. 89, p. 14, 2017.
[13] S. Das, H. Y. Chen, A. V. Penumatcha, and J. Appenzeller, "High performance multilayer MoS2 transistors with scandium contacts," *Nano Lett.*, vol. 13, no. 1, pp. 100–105, 2013.
[14] W. Zhang *et al.*, "Ultrahigh-gain photodetectors based on atomically thin graphene-MoS2 heterostructures.," *Sci. Rep.*, vol. 4, p. 3826, 2014.
[15] M. Bernardi, M. Palummo, and J. C. Grossman, "Extraordinary sunlight absorption and one nanometer thick photovoltaics using two-dimensional monolayer materials," *Nano Lett.*, vol. 13, no. 8, pp. 3664–3670, 2013.
[16] T. Roy *et al.*, "Field-effect transistors built from all two-dimensional material components," *ACS Nano*, vol. 8, no. 6, pp. 6259–6264, 2014.
[17] B. Radisavljevic and A. Kis, "Mobility engineering and a metal-insulator transition in monolayer MoS□.," *Nat. Mater.*, vol. 12, no. 9, pp. 815–20, 2013.
[18] Y. Wang *et al.*, "Buckling-Based Method for Measuring the Strain–Photonic Coupling Effect of GaAs Nanoribbons," *ACS Nano*, vol. 10 (9), pp. 8199–8206, 2016.
[19] C. Sealy, "GaAs nanoribbons take the strain," *Nano Today*, vol. 11, no. 5, pp. 539–540, Oct. 2016.

[20] B. P. Pandey, "Electronic and Transmission Properties of Low Buckled GaAs Armchair Nanoribbons," *J. Surf. Sci. Technol.*, vol. 33, no. (3–4), pp. 91–95, 2017.
[21] B. Mahler, V. Hoepfner, K. Liao, and G. A. Ozin, "Colloidal synthesis of 1T-WS2 and 2H-WS2 nanosheets: Applications for photocatalytic hydrogen evolution," *J. Am. Chem. Soc.*, vol. 136, no. 40, pp. 14121–14127, 2014.
[22] A. A. Balmashnov, K. S. Golovanivsky, E. M. Omeljanovsky, A. V Pakhomov, and A. Y. Polyakov, "Passivation of GaAs by atomic hydrogen flow produced by the crossed beams method," *Semicond. Sci. Technol.*, vol. 5, p. 242, 1990.
[23] H. Şahin *et al.*, "Monolayer honeycomb structures of group-IV elements and III-V binary compounds: First-principles calculations," *Phys. Rev. B - Condens. Matter Mater. Phys.*, vol. 80, no. 15, 2009.
[24] P. Giannozzi *et al.*, "QUANTUM ESPRESSO: a modular and open-source software project for quantum simulations of materials.," *J. Phys. Condens. Matter*, vol. 21, no. 39, p. 395502, 2009.
[25] J. Perdew, K. Burke, and Y. Wang, "Generalized gradient approximation for the exchange-correlation hole of a many-electron system," *Phys. Rev. B*, vol. 54, no. 23, pp. 16533–16539, 1996.
[26] K. Laasonen, R. Car, C. Lee, and D. Vanderbilt, "Implementation of ultrasoft pseudopotentials in ab initio molecular dynamics," *Phys. Rev. B*, vol. 43, no. 8, pp. 6796–6799, 1991.
[27] H. J. Monkhorst and J. D. Pack, "Special points for Brillouin-zone integrations," *Phys. Rev. B*, vol. 13, no. 12, pp. 5188–5192, 1976.
[28] "Atomistix ToolKit version 2016.2, QuantumWise A/S (www.quantumwise.com)." .
[29] F. Tran and P. Blaha, "Accurate Band Gaps of Semiconductors and Insulators with a Semilocal Exchange-Correlation Potential," *Phys. Rev. Lett.,* vol. 102, p. 226401, 2009.
[30] C. Hartwigsen, S. Goedecker, and J. Hutter, "Relativistic separable dual-space Gaussian pseudopotentials from H to Rn," *Phys. Rev. B*, vol. 58, p. 3641, 1998.
[31] W. A. Harrison, *Solid state theory*. New York: McGraw-Hill, 1970.
[32] R. M. Martin, "Electronic Structure: Basic Theory and Practical Methods," *Book*. p. 624, 2004.
[33] D. J. Griffiths, *Introduction to Electrodynamics*, 3rd ed. New Jersey: Prentice Hall, 1999.
[34] B. Herrmann, *Synthetic Methods of Organometallic and Inorganic Chemistry*, 2nd ed. New York: Georg Thieme Verlag Stuttgart, 1996.
[35] S. Adachi, *Handbook on Physical Properties of Semiconductors*. chichester: John Wiley &Sons, 2005.

In Press, Accepted Manuscript – Note to users

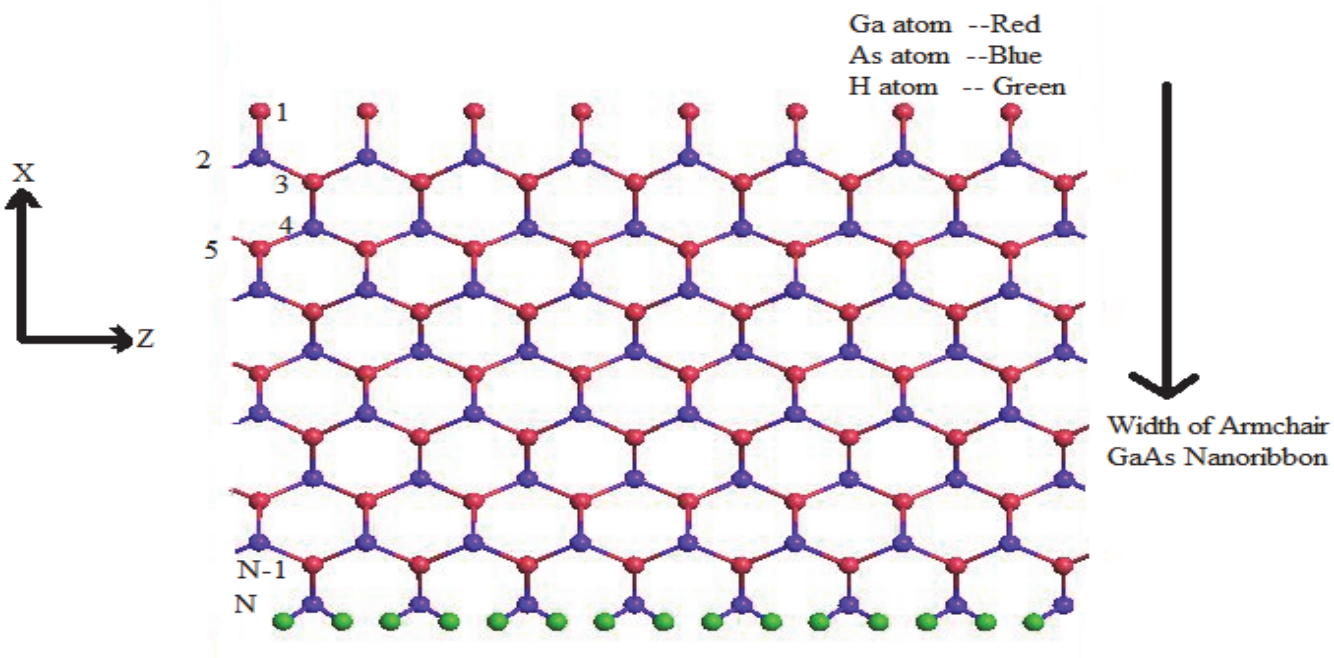

Fig. 1. Basic structure of buckled armchair GaAs nanoribbon.

In Press, Accepted Manuscript – Note to users

2a **2b**

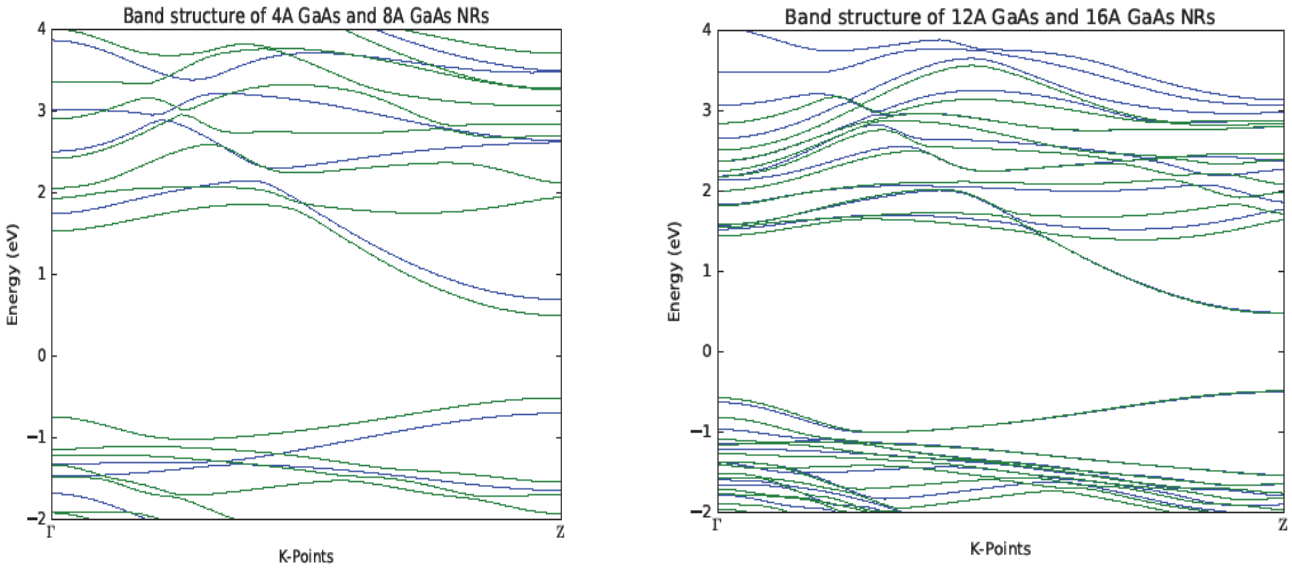

Fig. 2a, and 2b shows the band structure of N (4, 8), and N (12, 16) armchair GaAs Nanoribbons respectively. The band structure of 4A GaAs and 8A GaAs NRs are plotted in same Fig 2a with blue and green color, respectively. Fig 2b shows the band structure of 12A GaAs and 16A GaAs NRs with blue and green color, respectively. The calculated band structures of NA GaAs NRs predicts the direct bandgap nature of NA GaAs NRs at Γ(gamma), and decreases as the width of GaAs nanoribbons increases.

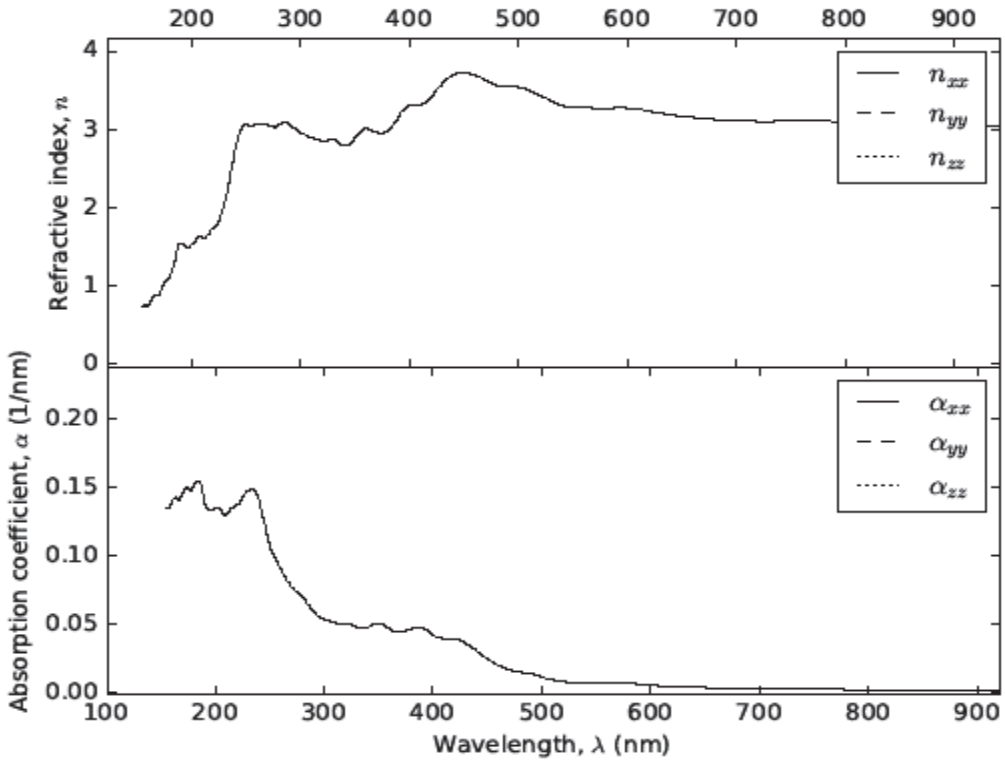

Fig. 3. Refractive index, n(ω) and absorption coefficient, $\alpha(\omega)$, calculated with complex dielectric constant for bulk zinc-blende GaAs.

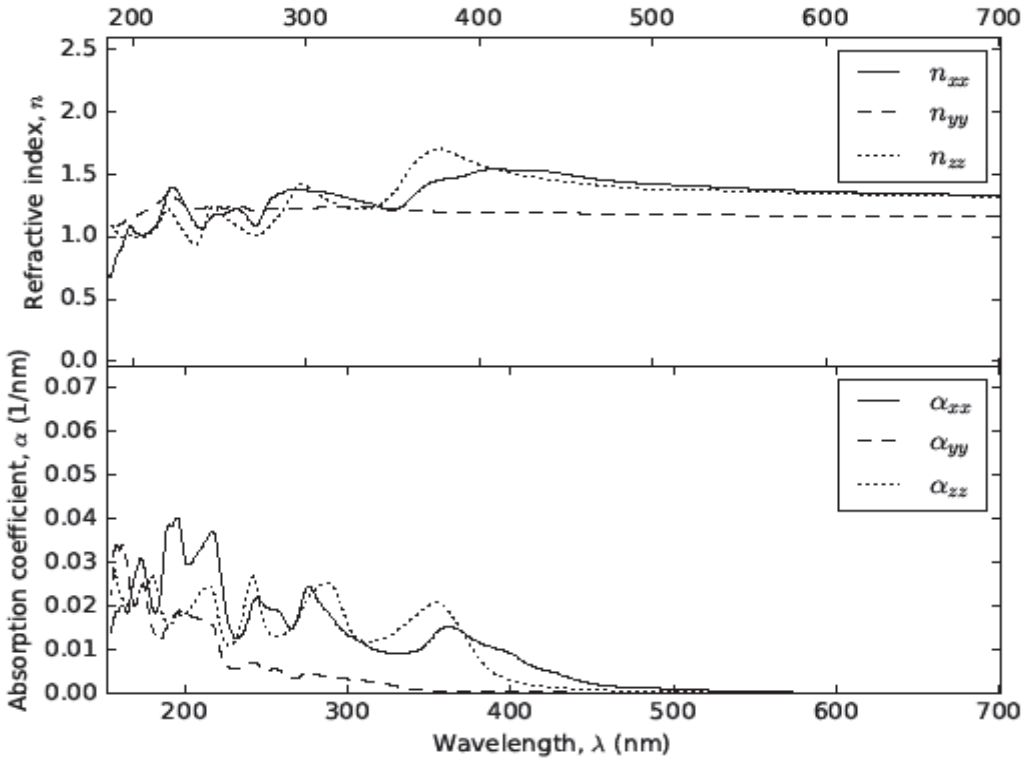

Fig. 4. Refractive index, n(ω) and absorption coefficient, $\alpha(\omega)$, calculated with complex dielectric constant for 4A GaAs NR.

In Press, Accepted Manuscript – Note to users

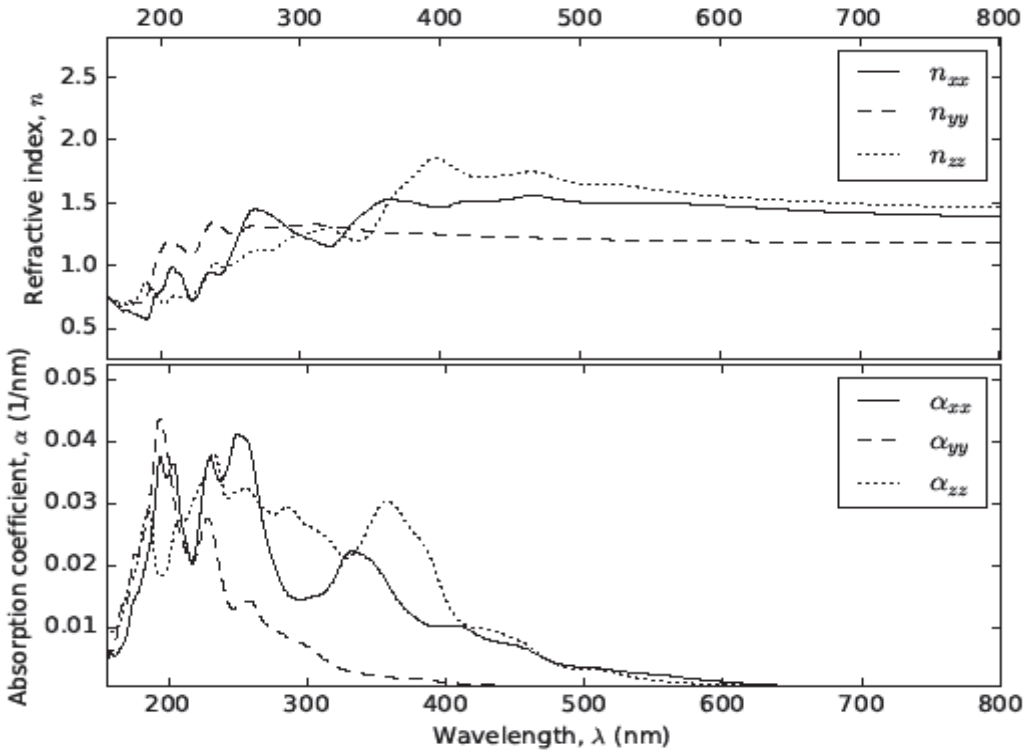

Fig. 5. Refractive index, n(ω) and absorption coefficient, $\alpha(\omega)$, calculated with complex dielectric constant for 8A GaAs NR.

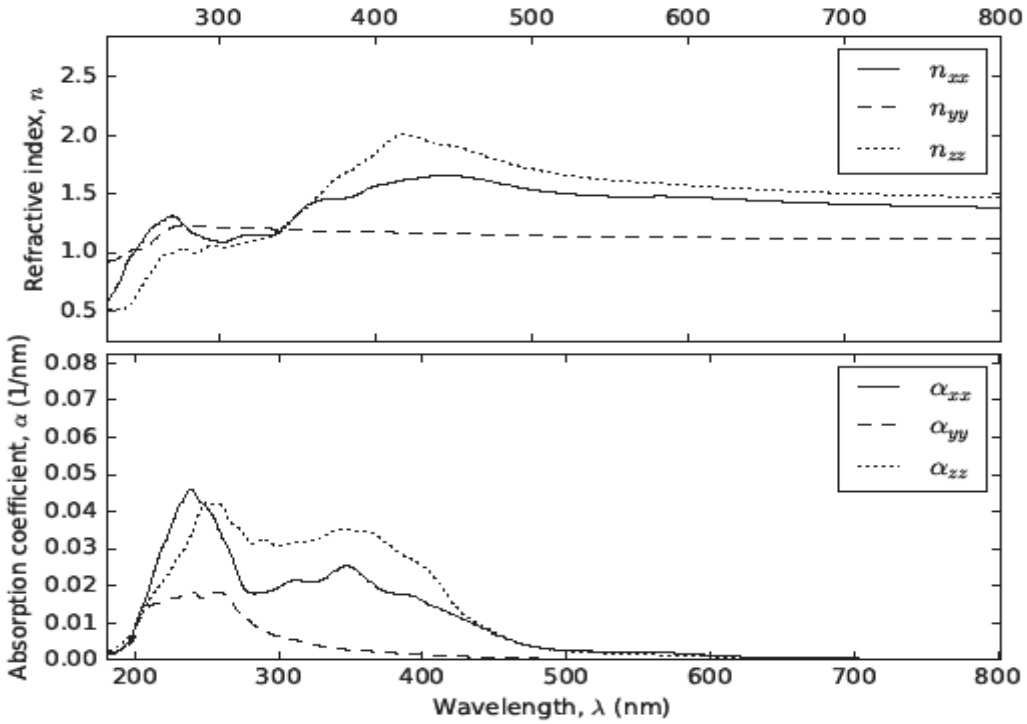

Fig. 6. Refractive index, n(ω) and absorption coefficient, $\alpha(\omega)$, calculated with complex dielectric constant for 12A GaAs NR.

In Press, Accepted Manuscript – Note to users

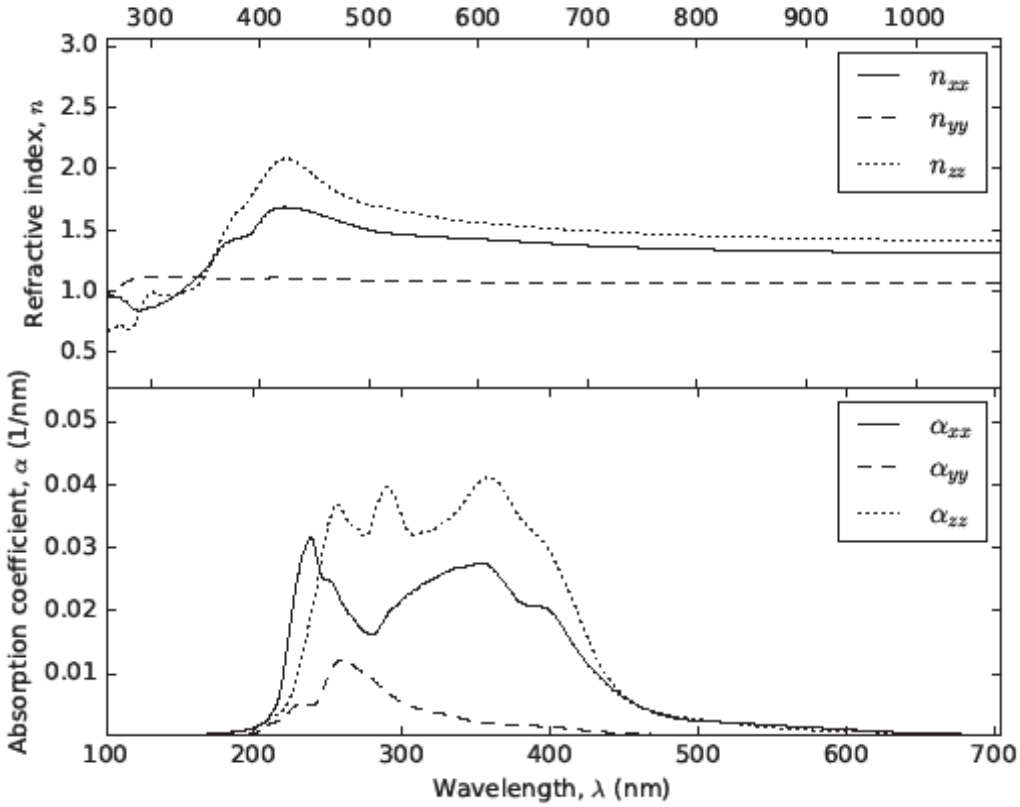

Fig. 7. Refractive index, n(ω) and absorption coefficient, $\alpha(\omega)$, calculated with complex dielectric constant for 16A GaAs NR.

Table 1. Bandgap (in eV) of NA GaAs NRs with a different width N: 4, 8, 12, 16. The bandgap of bulk GaAs has been calculated and compare with the experimental results.

Structure NA GaAs NRs	Fundamental direct bandgap (Z-Z)	Experimental Bandgap
Bulk GaAs	1.41	1.42[35]
4A GaAs NR	3.071	
8A GaAs NR	2.275	
12A GaAs NR	2.155	
16A GaAs NR	2.02	